Erzincan Üniversitesi
Fen Bilimleri Enstitüsü Dergisi
2022, 15(3), 684-698
ISSN: 1307-9085, e-ISSN: 2149-4584
Araştırma Makalesi

Erzincan University
Journal of Science and Technology
2022, 15(3), 684-698
DOI: 10.18185/erzifbed.1180213
Research Article

Removal of Congo Red From Water By Adsorption Onto Chitosan-BN-Fe_2O_3: Kinetic and Isotherm Studies

Mehmet Semih BİNGÖL[1*]

[1] Eastern Anatolia High Technology Application and Research Center (DAYTAM), Atatürk Üniversitesi, Erzurum/Turkey

Received:26/09/2022, **Revised:** 26/11/2022, **Accepted:** 09/12/2022, **Published:** 30/12/2022

Abstract

In this study, an adsorbent for Congo red removal was made by combining Chitosan and Boron Nitride(BN)-Fe_2O_3. The chemical structures of this adsorbent (Ch-BN-Fe_2O_3) were confirmed by FT-IR analysis. In adsorption studies, the effects of adsorbent amount, pH and contact time on Congo red removal were investigated. Accordingly, the highest 99.58% removal was achieved under the conditions of 0.1 gram adsorbent mass, pH 7, 60 minutes. In addition, thermodynamic, isotherm and kinetic studies were performed in the study. In isotherm studies, the most suitable model was determined to be Langmuir and its qmax value was found to be 86.95 mg/g. However, the pseudo second order kinetic model was found to be suitable.

Keywords: Chitosan, boron nitride, iron oxide, adsorption

Kongo Kırmızısının Kitosan-BN-Fe_2O_3 Üzerine Adsorpsiyon Yoluyla Sudan Uzaklaştırılması: Kinetik ve İzoterm Çalışmaları

Öz

Bu çalışmada Kongo red giderimi için Kitosana Boron Nitride- Fe_2O_3 katkılanıp adsorbent hazırlanmıştır. Bu adsorbentin (Ch-BN-Fe_2O_3) kimyasal yapıları FT-IR analizi ile doğrulanmıştır. Adsorpsiyon çalışmalarında adsorbent kütleleri, pH, temas süresi congo red giderimi üzerine etkileri araştırılmıştır. Buna göre 0,1 gram adsorbent kütlesi, pH 7, 60 dk sürede en yüksek %99,58 giderim gerçekleşmiştir. Ayrıca çalışmada termodinamik, izoterm ve kinetik çalışmalar gerçekleşmiştir. İzoterm çalışmalarında en uygun modelin langmuir olduğu belirlenmiş ve qmax değeri de 86,95 mg/g bulunmuştur. Bununla birlikte pseudo second order kinetic modeli uygun olduğu tespit edilmiştir.

Anahtar Kelimeler: Kitosan, bor nitrit, demir oksit, adsorpsiyon.

*Corresponding Author: semih.bingol@atauni.edu.tr
Mehmet Semih BİNGÖL, https://orcid.org/0000-0002-4616-7143

1. Introduction

Growing industrial waste as a result of technology advancements has had detrimental effects on the environment [1]. The rising usage of dyes and their discharge into environmental waters, particularly in numerous industrial applications, causes significant environmental and human health hazards[2,3]. Therefore, it is of great importance to treat these dyes before they are disposed of directly[4]. When these dyes are mixed with the surrounding waters, they cause many problems such as the increase of bacteria with sunlight and the prevention of biodegradation[5]. Congo red is the sodium salt of an acid called benzidinediazo-bis-1-naphthylamine-4-sulfonic acid. It is a secondary diazo (R-N=N-R bond) dye[6]. Congo red is frequently used in the textile, paper, printing, and plastic sectors despite having cancer- and mutagenic-causing qualities [7].

The removal of dyes from wastewater can be accomplished using a variety of physical/chemical techniques, including flocculation/coagulation[8], ion exchange electrochemistry[9], photochemical decomposition[10], reverse osmosis [11], ultrafiltration adsorption [12], chemical oxidation[13], and biological treatment techniques[14]. It has been seen in many studies that the most effective and economically most convenient of these methods is adsorption[15]. However, the materials utilized or created as adsorbents must be natural, safe for the environment, and capable of being easily separated from water[16].

The use of natural resources such as chitin and the biopolymer derived from it, chitosan, is becoming more and more important. In adsorption studies, the most important parameter is that the adsorbent is natural and harmless to the environment/human health. Chitosan was employed in this investigation due to this reason [17]. A biological polymer known as chitosan $(C_6H_{11}NO_4)n$ is derived from several natural sources[18]. In our investigation, boron nitride, an additive that doesn't harm the environment, was also used[19]. It is well known that many contaminants can be removed using boron nitride[20]. Because of its high surface area and chemically inert structure, boron nitride has become an essential material in pollution adsorption. In addition, Fe_2O_3 was added due to the active role of oxidized compounds in adsorbents[21]. Until now, there is a study in the literature on dye removal using chitosan/BN composite adsorbent. However, in this study, congo red was not removed and Fe_2O_3 was not added. Therefore, this study is unique in the literatüre [22]. Investigated were the effects of this produced adsorbent on congo red removal in various parameters.

2. Material and Methods

2.1. Preparation of BN-Fe_2O_3 doped chitosan adsorbent

Boron Nitride (Purity :%99.7, Nanography/Turkey), Chitosan (>%99), Fe_2O_3 (>%96), and Acetic acid (>%99) Sigma(St. Louis, Missouri, ABD) were purchased commercially. BN was treated with sodium hydroxide (NaOH), Due to the limited number of functional groups on its surface and chemical resistance [23]. For 24 hours at 120ºC, 1 gram of BN was mixed in the 5M NaOH. It was then washed and filtered numerous times with distilled water until the pH was restored. The resulting BNOH particles were dried at 60ºC for 10 hours. Fe_2O_3 (2g) and

prepared BNOH (0.5g) were mixed at 90ºC for 24 hours. The resulting particles were washed several times with distilled water and filtered. After that, it was dried for 10 hours at 60 ºC.

In 100 mL of 2% acetic acid solution, chitosan was completely dissolved. This solution was mixed for 24 hours with BN-Fe_2O_3 particles. Afterwards, the solution was kept at -80ºC for 24 hours and lyophilized. The resulting adsorbent was stored in a desicator. Fourier Transform Infrared Spectroscopy (FTIR) analysis was carried out using a Bruker VERTEX 70v model instrument in the scanning range of 400-4000 cm^{-1} in order to comprehend the chemical structures and bonding of adsorbents.

2.2. Adsorption Studies

Using various parameters conditions, a number of batch tests were conducted to look into the adsorption of Congo Red (CR) in produced adsorbents. These parameters are; dye concentration (50, 100, 150, 200 mg /L), pH levels (2–12) and mass of adsorbent (Ch-BN-Fe_2O_3) (0.01, 0.02, 0.03, 0.4, 0.05, 0.1, 0.15, 0.2 g/L) was determined. 1000 mg/L CR the stock solution was prepared to be diluted to the determined concentrations. Adsorption process was carried out by adding the determined amount of adsorbents into 50 ml of CR solution and running it at 150 rpm for the determined time in the IKA KS 3000i Control model shaker. The pH of the CR solution was adjusted using solutions of 0.1 M NaOH and 0.1 M HCl. After centrifugation, the adsorbents were removed from the solution. Using a colorimetric method, the remaining dye concentration in solution was determined using a UV spectrophotometer (Shimadzu UV-3600 Plus) (max wavelength 497.4 nm). An absorbance-concentration profile was constructed by drawing a calibration curve between dye solution absorbance and concentration. This graph is presented inn Figure 1. The formulas below were used to calculate the % removal of CR and the adsorption capacity of the adsorbent.

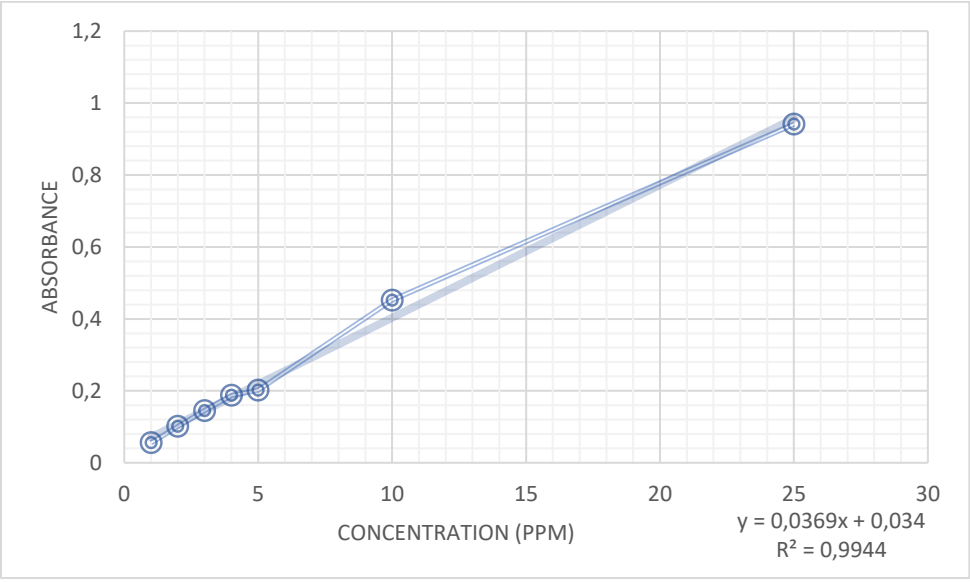

Figure 1. Congo red absorbance-concentration calibration curve

$$q_e = (c_0 - C_e) \times \frac{V}{W} \quad (1)$$

$$q_t = (c_0 - C_t) \times \frac{V}{W} \quad (2)$$

$$Removal, \% = \frac{(C_0 - C_e)}{C_0} \times 100 \quad (3)$$

Where C_0 is the initial concentration,C_e is equilibrium concentration and C_t is the concentration at time, q_e is equilibrium adsorption capacity and qt adsorption capacity at time, V is the volume of CR solution, and W is the adsorbent mass [24].

2.3. Adsorption Thermodynamics, Isotherm and Kinetic Studies

Adsorption studies were carried out thermodynamically at 3 different temperatures (298, 308, 318 Kelvin). With the use of the findings from these investigations, the following equations were used to derive Gibss, Enthalpy, and Entropy [25].

$$K_c = \frac{q_e}{C_e} \quad (4)$$

$$\ln K_c = \frac{\Delta S^0}{R} - \frac{\Delta H^0}{RT} \quad (5)$$

$$\Delta G^0 = \Delta H^0 - T\Delta S^0 \quad (6)$$

The adsorption isotherm is the most commonly used approach for representing an adsorption system's equilibrium state. The adsorption isotherm is the relationship between the amount of substance adsorbed by the adsorbent and the equilibrium concentration at constant temperature[26].

Equilibrium isotherm experiments were carried out at 25°C with 0.1 g adsorbent at pH 7 and different concentrations of CR (50-200 mg/L). The equilibrium adsorption values were analyzed using the Langmuir and Freundlich isotherm models.

The first adsorption isotherm to be formulated theoretically is the Langmuir isotherm equation. The majority of the later presented equations that successfully explain a variety of experimental findings are either based on this equation or were created utilizing the Langmuir method. As a result, both chemisorption and physical adsorption theories continue to benefit from the Langmuir isotherm model. The Langmuir isotherm can be expressed mathematically as follows[27].

$$\frac{C_e}{q_e} = \frac{1}{q_{max}\ K_c} + \frac{C_e}{q_{max}} \quad (7)$$

Where qmax, qe and Ce are respectively; Maximum adsorption capacity (mg/g), adsorption capacity at equilibrium (mg/g), equilibrium concentration (mg/L)

The Freundlich isotherm, another popular experimental equation that uses two parameters and is consisted with a wide range of experimental data, is similar to the Langmuir isotherm. The following equation serves as a representation of the Freundlich isotherm [28].

$$\ln q_e = \ln K_F + \left(\frac{1}{n}\right) \ln C_e \quad (9)$$

K_F and n are the Freundlich constants.

The effect of adsorbate-adsorbent contact time can be calculated using adsorption kinetics. There are steps in the analysis of adsorption kinetics that impact the rate of the adsorption process. In order to investigate the CR adsorption mechanism on adsorbent surfaces, two distinct kinetic models were applied. These two models are, respectively, pseudo-first-order kinetic models (PFO-km) and pseudo-second-order kinetic models (PSO-km) [27,29].

Lagergren created the PFO-km (1898). Eqn. 11 shows the PFO-km.

$$Log(q_e - q_t) = \ln q_e - \frac{K_1 t}{2.303} \quad (11)$$

The PSO-km is given in Eqn. 12 [30].

$$\frac{t}{q_t} = \frac{1}{k_2 q_e^2} + \frac{t}{q_e} \quad (12)$$

K_1 (min-1) and k_2 (g/mg min^{-1}) are the PFO-km constant and the PSO-km constant, respectively.

3. Results and Disscussion

3.1. FT-IR analysis

The chemical structure of the adsorbent was confirmed by FT-IR analysis. The Figure 2 shows the FT-IR spectrums of BN, Fe_2O_3, BN-Fe_2O_3 and Ch-BN-Fe_2O_3. In BN spectrums, 1332 cm^{-1} BN stretch vibration and 771 cm^{-1} peak indicate B-N-B formation[31]. In the Fe_2O_3 FTIR analysis, the 698 and 546 peaks show the Fe_2O_3 tension, and 420 cm^{-1} shows the Fe_2O_3 bending vibration[32]. Both BN and Fe_2O_3 have similar peaks in the BN-Fe_2O_3 analysis[33]. Ch-BN-Fe_2O_3 adsorbent originates from the Fe-O group at 611 cm-1, the NH_2 absorption of chitosan at 1560 and 1654 cm^{-1} and the C=O amide group. In addition, the 3268 and 2917 cm^{-1} peaks originate from the OH- group[34,35]. In the FT-IR analysis of the adsorbent, the specific peaks of BN and Fe_2O_3 are seen similarly, although there are small shifts.

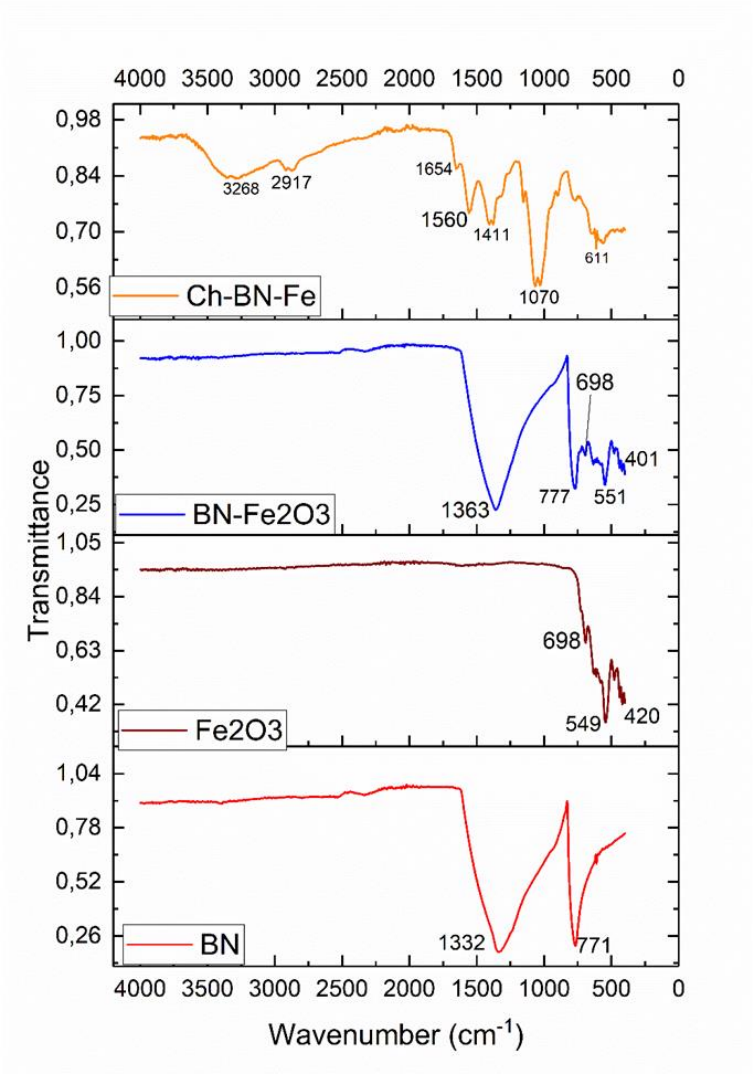

Figure 2. FT-IR spectra of the adsorbent

3.2. Effect of amount Ch-BN-Fe_2O_3

Firstly, the impact of adsorbent masses was assessed in the adsorption studies. The adsorption studies was performed in 120 min., at 25 ºC, pH 7, and 100 mg/L CR concentration. According to Figure 3, the maximum CR adsorption removal was determined to be 99.06%. As the adsorbent amount is increased, the adsorption increased and remained constant after 0.1 gram.

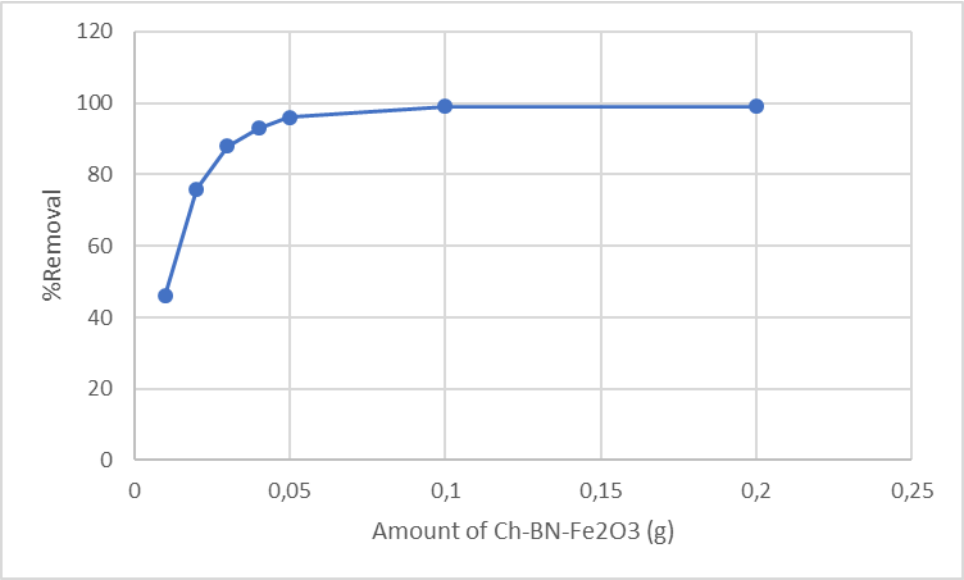

Figure 3. The effect of Ch-BN-Fe_2O_3 amount on adsorption.

3.3. Effect of pH on adsorption

The impact of pH on adsorption was investigated. The adsorption study was carried out for 120 min., at a temperature of 25 ºC, using 0.1 grams of adsorbent and 100 mg/L of CR concentration. As shown in the Figure 4 that percentage of CR removal remained steady until pH 7, but then declined. According to the results, the highest CR removal was found to be 99.04% at pH 7[36].

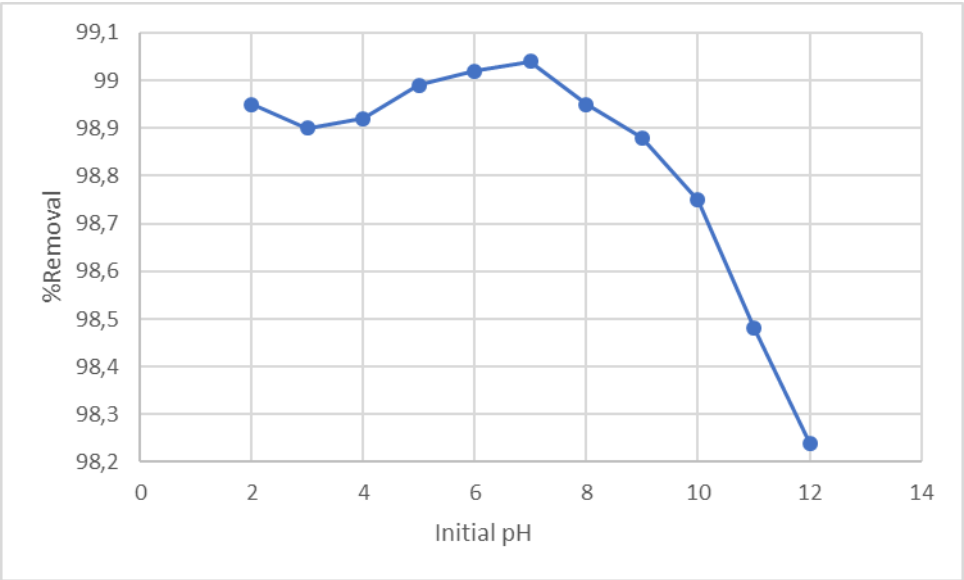

Figure 4. Effect of pH on CR removal

3.4. Effect of contact time and initial concentration

Figure 5 shows the effect of time and initial concentration on adsorption. These experiments were performed under conditions that a temperature of 25°C, using 0.1 grams of adsorbent and

pH 7. Accordingly, very fast adsorption took place up to 20 minutes and then remained stable. This results from the active sites on the adsorbent surface being filled. The highest CR removal was found to be 99.58% at 50 ppm initial concentration. The highest adsorption capacity was determined as 85 mg/g at an initial concentration of 200 ppm.

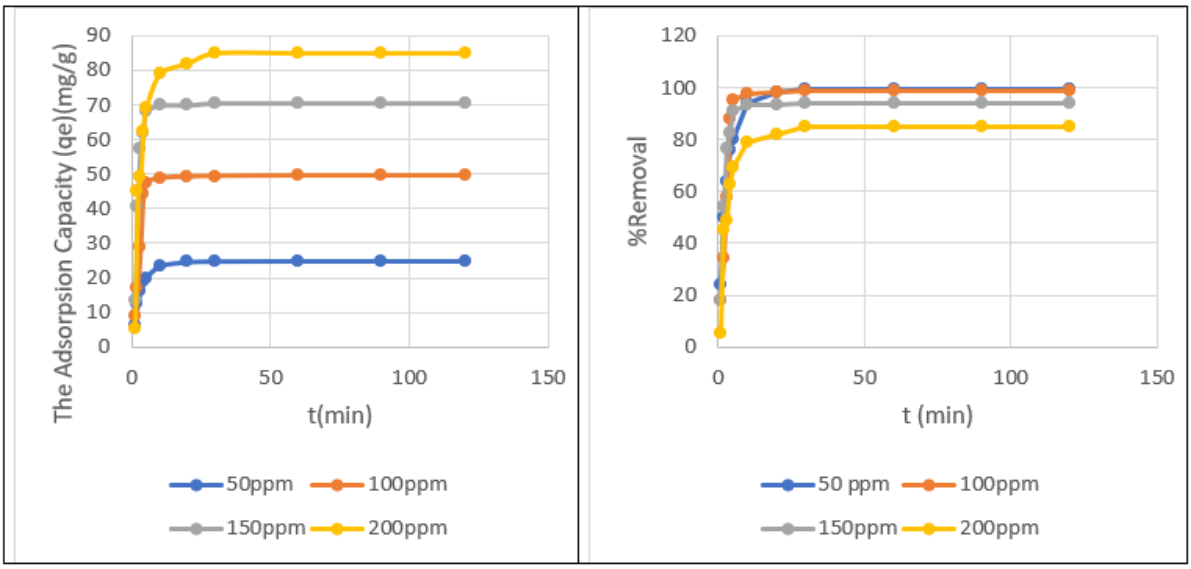

Figure 5. The effect of initial dye concentration and time on adsorption: (a) CR removal rate and (b) the amount of CR adsorbed at equilibrium

3.5. Results of Thermodynamic, Isotherm and Kinetic studies

Experiments were conducted at 100 ppm CR concentration, for 60 minutes, at pH 7, and under the circumstances of 0.1gram adsorbent amount in order to study the effect of temperature and thermodynamic studies. It was observed that as the temperature increases, the adsorption increased slightly. Thermodynamic parameters were calculated with the help of Figure 6 and 7. Parameter results are presented in Table 1. At all temperatures, negative values of ΔG (-11.46, -11.68, and -12.1 kJ/mol) show that the reaction is spontaneous. In general, physisorption is represented by ΔG values of $-20 < \Delta G < 0$ (kJ/mol). Additionally, it was shown that ΔG fell as temperature rose, demonstrating the viability of adsorption at higher temperatures. Positive enthalpy (ΔH= 1.257 kJ/mol) indicates endothermic adsorption. Positive entropy (ΔS = 0.042 kJ/mol) indicates increased randomness during adsorption at the solid-solution interface[37].

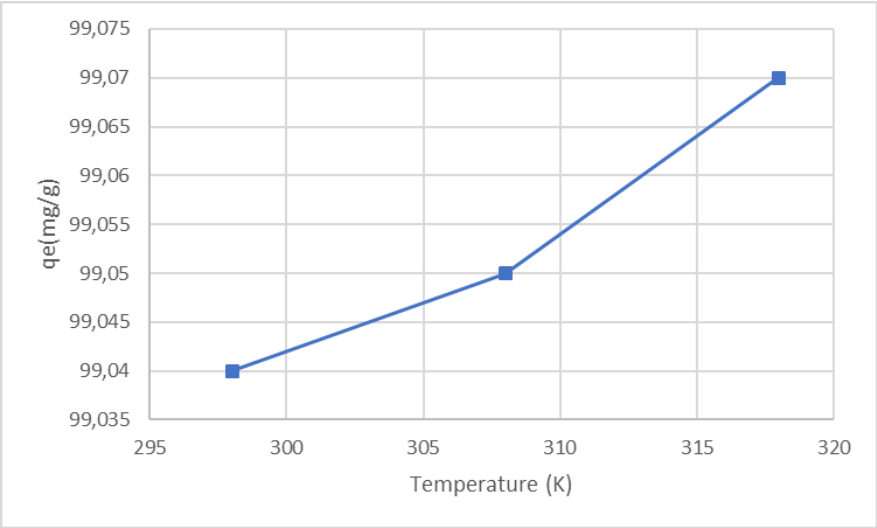

Figure 6. Effect of temperature on adsorption

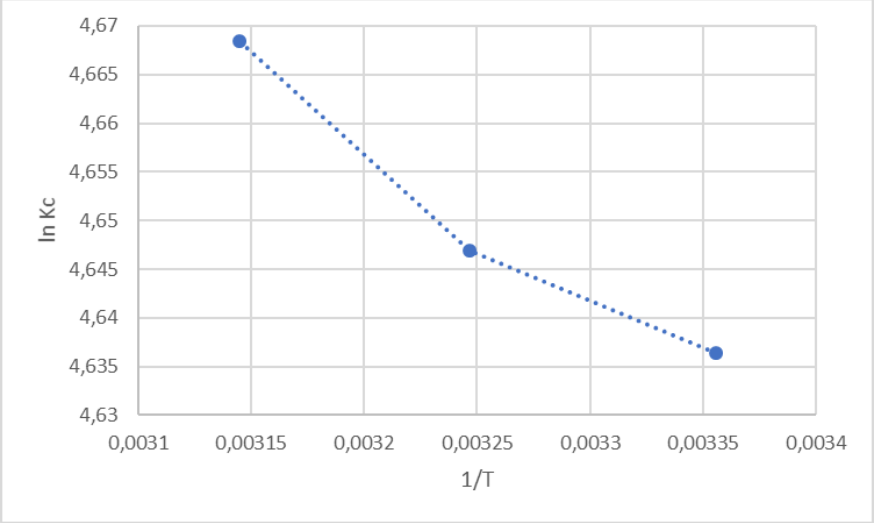

Figure 7. lnKc versus 1/T

Table 1. Thermodynamic parameters for CR adsorption

T (Kelvin)	ΔH (kJ/mol)	ΔS (kJ/mol)	ΔG (kJ/mol K)
298	1.257	0.042	-11.46
308	1.257	0.042	-11.68
318	1.257	0.042	-12.1

The values of the Langmuir and Freundlich model parameters for CR adsorption by the produced adsorbent are shown in Table 2 and Figure 8. Comparison of these two models showed that the Langmuir model with R^2> 0.99 was a better match than the Freundlich model

(R^2=0.9289). This showed that adsorption mechanism is compatible with the Langmuir isotherm. This demonstrates that CR is adsorbed as a single layer coating on the surface[38].

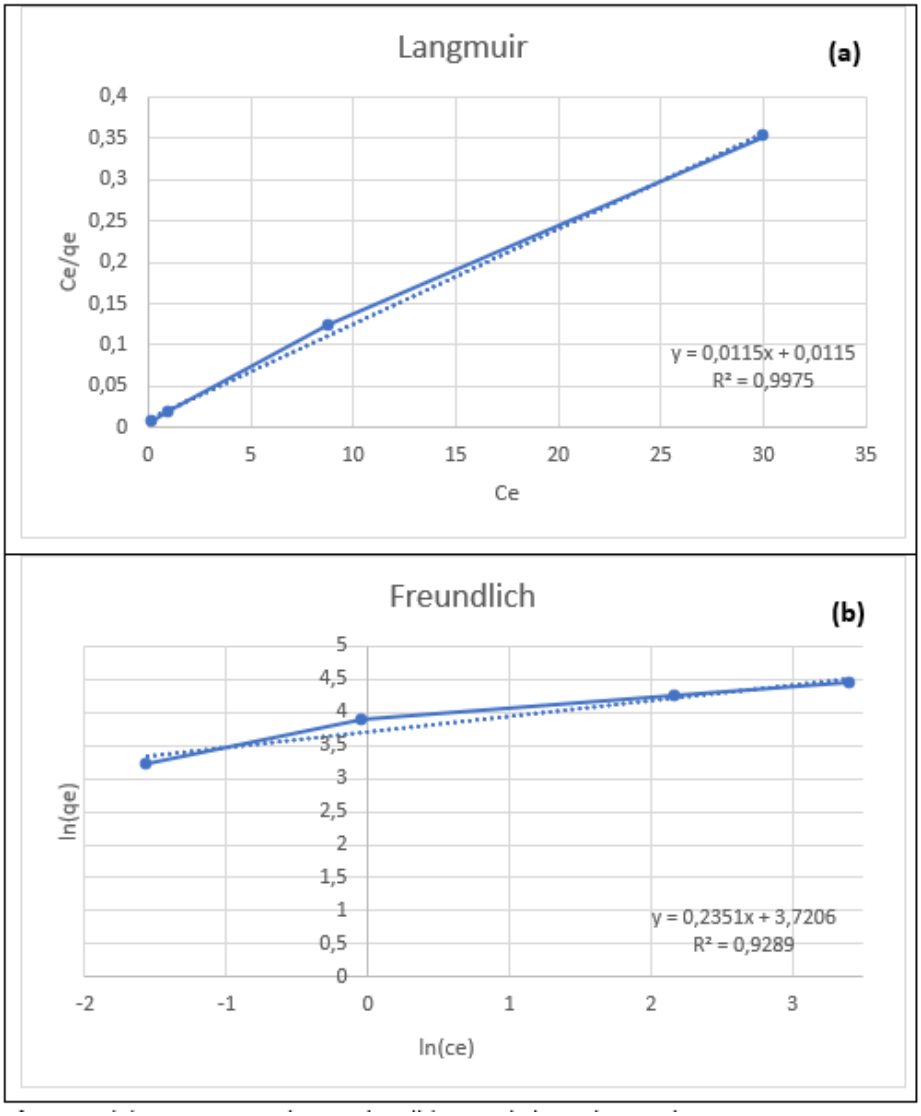

Figure 8. (a) Langmuir Isotherm Plot, **(b)** Freunlich Isotherm Plot

Table 2. Isotherm models parameters results.

Isotherm	Parameters	Value
Langmuir	R^2	0.9975
	q_{max}(mg/g)	86.95
	K_L	1.01
Freundlich	R^2	0.9289
	K_F (L/mg)	41.28
	n	0.25

The experimentally collected data were used to apply the linear forms of the PFO and PSO velocity models in order to examine the adsorption control mechanism. Table 3 and Figure 9

contain the data and graphs for the kinetic parameter results. Experimental findings are compatible with PSO. The PSO fit was further demonstrated by the R^2 value of 0.999. As seen in the Table 4, when the experimental results and the results in pso were compared, it was seen that they were very close to each other. This showed that adsorption study is suitable for the PSO model. Improved and experimental kinetic velocity profiles further supported this. As a result, the rate-controlling step for this adsorbent is probably chemical adsorption[39].

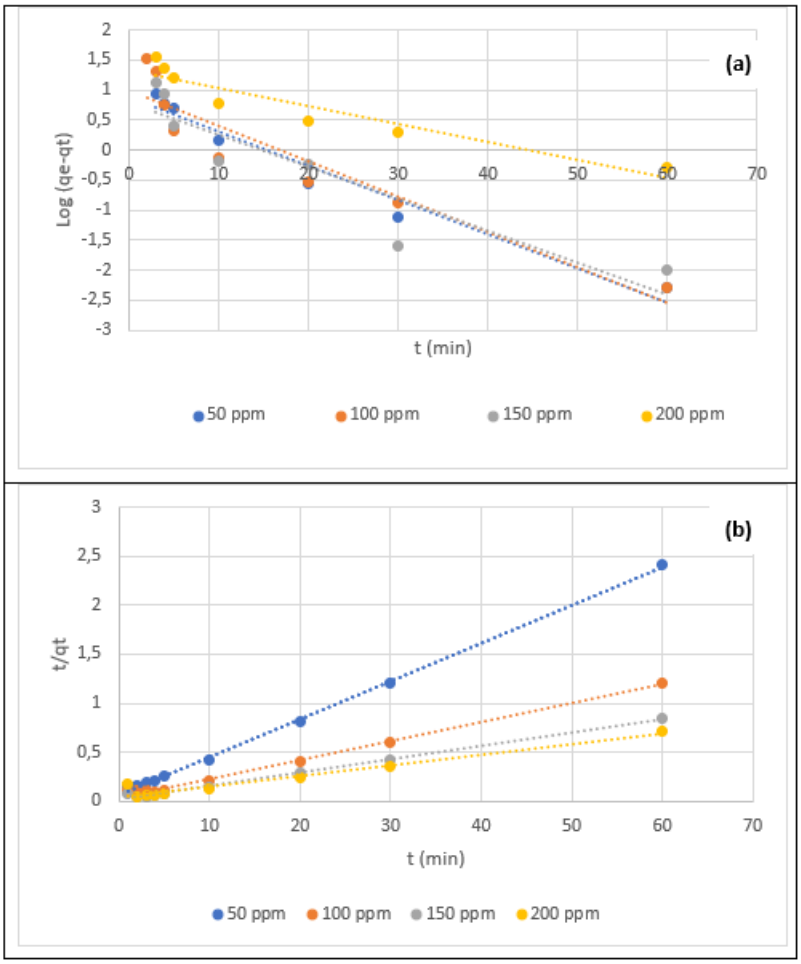

Figure 9. (a) PFO and (b) PSO kinetics plots of CR.

Table 4. The results of the kinetic parameters for CR adsorption

		PFO-km			PSO-km		
Co (mg/L)	**q_{exp}(mg/g)**	**q_e (mg/g)**	**K_1**	**R^2**	**q_e (mg/g)**	**K_2**	**R^2**
50	24,89	2,56	0,134	0.9584	25,9	0.0238	0.9985
100	49,52	3,08	0,142	0.8755	52,08	0.0091	0.9935
150	70,6	2,18	0,122	0,8305	72,99	0.0102	0.9958
200	85	3,79	0,069	0,8407	88,15	0.0073	0.9996

4. Conclusion

Chitosan doped with BN-Fe_2O_3 that was utilized to remove CR was created for the first time in the literature. By using FT-IR analysis, the produced adsorbent's chemical structures were verified. Adsorption studies have shown that 0.1 g of adsorbent, pH 7, and 60 minutes of adsorption time are the best conditions. It was discovered that the Langmuir isotherm model was appropriate for this adsorption. The qmax value was also discovered to be 85 mg/g. The kinetic studies led to the conclusion that the PSO-km was appropriate..

Ethics in Publishing

There are no ethical issues regarding the publication of this study.

References

[1] Harja, M., Buema, G., & Bucur, D. (2022) Recent advances in removal of Congo Red dye by adsorption using an industrial waste. Scientific Reports., *12*(1), 1–18

[2] Zhang, H., Chen, H., Azat, S., Mansurov, Z. A., Liu, X., Wang, J., Su, X., et al. (2018) Super adsorption capability of rhombic dodecahedral Ca-Al layered double oxides for Congo red removal. Journal of Alloys and Compounds., *768*, 572–581

[3] Cheng, Y., Yan, F., Huang, F., Chu, W., Pan, D., Chen, Z., Zheng, J., et al. (2010) Bioremediation of Cr (VI) and immobilization as Cr (III) by Ochrobactrum anthropi. Environmental science & technology., *44*(16), 6357–6363

[4] You, J., Liu, C., Feng, X., Lu, B., Xia, L., & Zhuang, X. (2022) In situ synthesis of ZnS nanoparticles onto cellulose/chitosan sponge for adsorption–photocatalytic removal of Congo red. Carbohydrate Polymers., *288*, 119332

[5] Eltaweil, A. S., Elshishini, H. M., Ghatass, Z. F., & Elsubruiti, G. M. (2021) Ultra-high adsorption capacity and selective removal of Congo red over aminated graphene oxide modified Mn-doped UiO-66 MOF. Powder technology., *379*, 407–416

[6] Mandal, S., Calderon, J., Marpu, S. B., Omary, M. A., & Shi, S. Q. (2021) Mesoporous activated carbon as a green adsorbent for the removal of heavy metals and Congo red: Characterization, adsorption kinetics, and isotherm studies. Journal of Contaminant Hydrology., *243*, 103869

[7] Parvin, S., Biswas, B. K., Rahman, M. A., Rahman, M. H., Anik, M. S., & Uddin, M. R. (2019) Study on adsorption of Congo red onto chemically modified egg shell membrane. Chemosphere., *236*, 124326

[8] Lee, J.-W., Choi, S.-P., Thiruvenkatachari, R., Shim, W.-G., & Moon, H. (2006) Submerged microfiltration membrane coupled with alum coagulation/powdered activated carbon adsorption for complete decolorization of reactive dyes. Water research., *40*(3), 435–444

[9] Gu, J., Liu, H., Wang, S., Zhang, M., & Liu, Y. (2019) An innovative anaerobic MBR-reverse osmosis-ion exchange process for energy-efficient reclamation of municipal

wastewater to NEWater-like product water. Journal of Cleaner Production., *230*, 1287–1293

[10] Qi, L., Yu, J., & Jaroniec, M. (2013) Enhanced and suppressed effects of ionic liquid on the photocatalytic activity of TiO2. Adsorption., *19*(2), 557–561

[11] Atab, M. S., Smallbone, A. J., & Roskilly, A. P. (2018) A hybrid reverse osmosis/adsorption desalination plant for irrigation and drinking water. Desalination., *444*, 44–52

[12] Naddeo, V., Secondes, M. F. N., Borea, L., Hasan, S. W., Ballesteros Jr, F., & Belgiorno, V. (2020) Removal of contaminants of emerging concern from real wastewater by an innovative hybrid membrane process–UltraSound, Adsorption, and Membrane ultrafiltration (USAMe®). Ultrasonics Sonochemistry., *68*, 105237

[13] Michael-Kordatou, I., Karaolia, P., & Fatta-Kassinos, D. (2018) The role of operating parameters and oxidative damage mechanisms of advanced chemical oxidation processes in the combat against antibiotic-resistant bacteria and resistance genes present in urban wastewater. Water research., *129*, 208–230

[14] Nancharaiah, Y. V, & Sarvajith, M. (2019) Aerobic granular sludge process: a fast growing biological treatment for sustainable wastewater treatment. Current Opinion in Environmental Science & Health., *12*, 57–65

[15] Rashid, R., Shafiq, I., Akhter, P., Iqbal, M. J., & Hussain, M. (2021) A state-of-the-art review on wastewater treatment techniques: the effectiveness of adsorption method. Environmental Science and Pollution Research., *28*(8), 9050–9066

[16] Velusamy, S., Roy, A., Sundaram, S., & Kumar Mallick, T. (2021) A review on heavy metal ions and containing dyes removal through graphene oxide-based adsorption strategies for textile wastewater treatment. The Chemical Record., *21*(7), 1570–1610

[17] Saheed, I. O., Oh, W. Da, & Suah, F. B. M. (2021) Chitosan modifications for adsorption of pollutants–A review. Journal of hazardous materials., *408*, 124889

[18] Qamar, S. A., Ashiq, M., Jahangeer, M., Riasat, A., & Bilal, M. (2020) Chitosan-based hybrid materials as adsorbents for textile dyes–A review. Case Studies in Chemical and Environmental Engineering., *2*, 100021

[19] Yu, S., Wang, X., Pang, H., Zhang, R., Song, W., Fu, D., Hayat, T., et al. (2018) Boron nitride-based materials for the removal of pollutants from aqueous solutions: a review. Chemical Engineering Journal., *333*, 343–360

[20] Li, J., Xiao, X., Xu, X., Lin, J., Huang, Y., Xue, Y., Jin, P., et al. (2013) Activated boron nitride as an effective adsorbent for metal ions and organic pollutants. *Scientific reports*., *3*(1), 1–7

[21] Ouyang, J., Zhao, Z., Suib, S. L., & Yang, H. (2019) Degradation of Congo Red dye by a Fe2O3@ CeO2-ZrO2/Palygorskite composite catalyst: synergetic effects of Fe2O3. Journal of colloid and interface science., *539*, 135–145

[22] Khose, R. V, Lokhande, K. D., Bhakare, M. A., Dhumal, P. S., Wadekar, P. H., & Some,

S. (2021) Boron Nitride doped Chitosan Functionalized Graphene for an Efficient Dye Degradation. ChemistrySelect., *6*(31), 7956–7963

[23] Kim, K., Ju, H., & Kim, J. (2016) Surface modification of BN/Fe3O4 hybrid particle to enhance interfacial affinity for high thermal conductive material. Polymer., *91*, 74–80

[24] Kavci, E., Erkmen, J., & Bingöl, M. S. (2021) Removal of methylene blue dye from aqueous solution using citric acid modified apricot stone. Chemical Engineering Communications., 1–16

[25] Mondal, N. K., & Kar, S. (2018) Potentiality of banana peel for removal of Congo red dye from aqueous solution: isotherm, kinetics and thermodynamics studies. Applied Water Science., *8*(6), 1–12

[26] Wekoye, J. N., Wanyonyi, W. C., Wangila, P. T., & Tonui, M. K. (2020) Kinetic and equilibrium studies of Congo red dye adsorption on cabbage waste powder. Environmental Chemistry and Ecotoxicology., *2*, 24–31

[27] Lagergren, S. K. (1898) About the theory of so-called adsorption of soluble substances. Sven. Vetenskapsakad. Handingarl., *24*, 1–39

[28] Proctor, A., & Toro-Vazquez, J. F. (1996) The Freundlich isotherm in studying adsorption in oil processing. Journal of the American Oil Chemists' Society., *73*(12), 1627–1633

[29] Hubbe, M. A., Azizian, S., & Douven, S. (2019) Implications of apparent pseudo-second-order adsorption kinetics onto cellulosic materials: A review. BioResources., *14*(3)

[30] Ho, Y.-S., & McKay, G. (1999) Pseudo-second order model for sorption processes. Process biochemistry., *34*(5), 451–465

[31] Wei, R., Xiao, Q., Zhan, C., You, Y., Zhou, X., & Liu, X. (2019) Polyarylene ether nitrile and boron nitride composites: coating with sulfonated polyarylene ether nitrile. e-Polymers., *19*(1), 70–78

[32] Sobhanardakani, S., Jafari, A., Zandipak, R., & Meidanchi, A. (2018) Removal of heavy metal (Hg(II) and Cr(VI)) ions from aqueous solutions using Fe2O3@SiO2 thin films as a novel adsorbent. Process Safety and Environmental Protection., *120*, 348–357

[33] Thangasamy, P., & Sathish, M. (2018) Dwindling the re-stacking by simultaneous exfoliation of boron nitride and decoration of α-Fe2O3 nanoparticles using a solvothermal route. New Journal of Chemistry., *42*(7), 5090–5095

[34] Zhu, H.-Y., Jiang, R., Xiao, L., & Li, W. (2010) A novel magnetically separable γ-Fe2O3/crosslinked chitosan adsorbent: Preparation, characterization and adsorption application for removal of hazardous azo dye. Journal of Hazardous Materials., *179*(1), 251–257

[35] Dhanavel, S., Sivaranjani, T., Sivakumar, K., Palani, P., Gupta, V. K., Narayanan, V., & Stephen, A. (2021) Cross-linked chitosan/hydroxylated boron nitride nanocomposites for co-delivery of curcumin and 5-fluorouracil towards human colon cancer cells. Journal of the Iranian Chemical Society., *18*(2), 317–329

[36] Kavci, E. (2021) Malachite green adsorption onto modified pine cone: Isotherms, kinetics and thermodynamics mechanism. Chemical Engineering Communications., *208*(3), 318–327

[37] Wakkel, M., Khiari, B., & Zagrouba, F. (2019) Textile wastewater treatment by agro-industrial waste: Equilibrium modelling, thermodynamics and mass transfer mechanisms of cationic dyes adsorption onto low-cost lignocellulosic adsorbent. Journal of the Taiwan Institute of Chemical Engineers., *96*, 439–452

[38] Mahmoud, M. S., & Mahmoud, A. S. (2021) Wastewater treatment using nano bimetallic iron/copper, adsorption isotherm, kinetic studies, and artificial intelligence neural networks. Emergent Materials., *4*(5), 1455–1463

[39] Hasanzadeh, M., Simchi, A., & Far, H. S. (2020) Nanoporous composites of activated carbon-metal organic frameworks for organic dye adsorption: Synthesis, adsorption mechanism and kinetics studies. Journal of Industrial and Engineering Chemistry., *81*, 405–414